Journal Homepage: http://ijcpe.uobaghdad.edu.iq
Iraqi Journal of Chemical and Petroleum Engineering
Vol. 26 No. 4 (December 2025) 89 – 95
EISSN: 2618-0707, PISSN: 1997-4884

Experimental study of gas-brine capillarity measurement at high temperature and pressure

Hiwa Sidiq [a, *]

a Komar University of Science and Technology, Sulaimani, Kurdistan Region, Iraq

Abstract

Understanding capillary pressure profiles during gas-brine coreflooding is essential for analyzing fluid behavior in porous media, particularly in gas reservoirs. Direct measurement of capillary pressure in dynamic displacement experiments relies on evaluating the balance between capillary forces and pressure gradients within the porous structure. In this experimental study three rock samples were taken from a natural gas reservoir located on Australia's Northwest Shelf. Experiments were conducted under simulated reservoir conditions (~ 41.37 MPa and 368.15 K) to investigate the effects of pore size, porosity, and water saturation on the capillary pressure profile. The capillary pressure curves (Samples C1–C3) reveal distinct dynamic behaviors. Samples C1 and C2, which have higher permeability and porosity, exhibit an initial decrease followed by a monotonic rise in capillary pressure until breakthrough. In contrast, Sample C3, characterized by lower permeability and porosity, shows lower brine saturation. However, higher brine saturation would typically be expected in low-porosity samples due to increased grain surface area and smaller pore throats that trap the wetting phase. This unexpected result is attributed to the experiments being conducted under high-pressure and high-temperature conditions. These findings underscore the critical role of pore geometry in governing displacement efficiency and capillary trapping. They also provide valuable quantitative insights for reservoir modeling, particularly in predicting gas recovery under HPHT conditions where capillary forces are significant.

Keywords: Capillary Pressure; Coreflooding; HPHT; Gas Reservoir.

Received on 03/09/2025, Received in Revised Form on 23/11/2025, Accepted on 25/11/2025, Published on 30/12/2025

https://doi.org/10.31699/IJCPE.2025.4.8

1- Introduction

Capillary pressure (P_c) measurement in reservoir sandstone is fundamental for understanding multiphase flow behavior, particularly in low permeability gas reservoirs**,** where capillary and interfacial forces dominate fluid transport [1]. In such tight formations, gas flow from the matrix to the wellbore occurs at low rates, often governed by the rock's capillary pressure profile. Accurate P_c data are critical for predicting fluid distribution, relative permeability, and phase trapping under reservoir conditions [2]. These parameters are essential to assess whether economical gas production is feasible, especially in unconventional gas plays where production relies on matrix-to-fracture flow.

Capillary pressure is intrinsically linked to pore size distribution (PSD)**,** grain size, and pore geometry. Larger pores require lower capillary pressures for non-wetting phase invasion, whereas smaller pores need significantly higher pressures. Consequently, the shape of the capillary pressure curve can provide insights into the PSD and rock quality, influencing estimates of irreducible water saturation (S_{wr}) and residual gas saturation (S_{gr}) [3–5]. Various methods have been developed to measure P_c, including mercury injection**,** centrifuge**,** porous plate**,** and dynamic coreflooding techniques. Among them, dynamic P_c measurement under high pressure and high temperature (HPHT) conditions is particularly important, as it reflects realistic reservoir conditions and incorporates viscous and capillary effects [6, 7]. Furthermore, Das, [8] conduct experiments to quantify the dynamic effect in porous media, revealing that dynamic capillary pressure relationships differ from static ones, especially under varying flow conditions. Their findings support the necessity of incorporating dynamic P_c measurements to capture realistic reservoir behaviors. It also helps determine relative permeability curves more accurately, which are essential for reservoir simulation and production planning. Moreover, comprehensive studies of the dynamic capillary pressure effects in porous media, particularly in low-permeability and tight reservoirs, were conducted by Li et al. [9]. Their study emphasizes the mechanisms and significance of dynamic capillarity in non-equilibrium flow.

Due to the complexity of fluid flow in heterogeneous and tight formations, no single technique can capture the complete P_c curve. For example, porous plate methods are often used for low-pressure drainage data, while dynamic gas-brine displacement is required for HPHT conditions, simulating actual field operations [10, 11]. Gas injection under HPHT may lead to gas dissolution in the brine, reducing capillary contrast and influencing recovery

*Corresponding Author: Email: hiwa.sidiq@komar.edu.iq

factors and S_{wr}. Additionally, in some enhanced gas recovery strategies, gas injection is used to vaporize formation water, but this can result in salt precipitation, impairing permeability [12, 13]. Understanding this requires an accurate P_c curve that reflects the wettability, interfacial tension (IFT), and phase behavior of the rock-fluid system.

Grain and pore size, surface wettability, and heterogeneity affect how gas displaces water, the development of residual saturations, and the overall production efficiency. The primary difference is that oil reservoirs are generally oil-wet or intermediate-wet, resulting in distinct pore-scale capillary forces. This variation significantly diminishes the effectiveness of capillary trapping [14]. High IFT and unfavorable viscosity ratios in gas-brine systems can hinder displacement, leaving behind substantial water or gas. Capillary pressure data are therefore indispensable in reservoir simulation, helping predict relative permeability**,** phase distributions**,** and long-term gas recovery [15–18]. Incorporating P_c data improves modeling of gas mobility, especially in heterogeneous formations where pore throats and wettability alter displacement patterns [19]. Thus, comprehensive capillary pressure characterization—especially via dynamic methods under HPHT—remains a cornerstone for optimizing gas reservoir performance and recovery strategies**.**

Understanding capillary pressure under HPHT conditions is crucial for accurately predicting fluid behavior and flow in reservoirs. However, most P_c studies are limited to ambient or low-pressure conditions. Currently, there's a clear lack of experimental P_c data at HPHT (> 35 MPa and > 363 ^{0}K), a significant gap that this work aims to address.

A detailed analysis of the pressure differential versus injected pore volume and water saturation is presented in this paper. To maintain consistent experimental conditions, the injection velocity was kept constant and low flowrate for each core: 9.9 cm/hr for core C1, 10.7 cm/hr for core C2, and 10.8 cm/hr for core C3.

2- Experimental setup

The dynamic method was used to generate gas-brine capillary pressure data. As shown in Fig. 1, the key components of the dynamic rig were an injection and collection unit, a core holder, a backpressure regulator to maintain the desired pressure conditions, and an air bath for temperature control. Additionally, injection rates were carefully measured at both the inlet and outlet ends of the core holder.

The displacing phases were stored in titanium accumulators connected to syringe pump. To simulate reservoir conditions, the fluids were pre-heated in an air bath, and the procedure began by saturating the core plugs with 25,000 ppm brine, followed by gas injection to initiate displacement. During the process, differential pressure, injected pore volumes, and saturation changes were carefully recorded. Temperature was precisely controlled using a high-precision thermocouple, while differential pressure was continuously monitored by high-accuracy pressure transducers, digitally synchronized with a laboratory computer for data acquisition.

3- Experimental design

The core plugs were placed inside a Viton Hassler sleeve within the core holder, then evacuated and saturated with connate water. They were subsequently flushed with more than 10 pore volumes of brine before gas injection. A gas mixture consisting of 90% methane and 10% CO_2 (as recommended by Shell Australia) was injected to displace the brine to connate water saturation. The composition of the produced gas was continuously monitored using a PEM Tech CO_2 gas analyzer, with real-time data streamed to a laboratory computer. The volume of produced gas was measured using a calibrated flow meter.

The experimental procedure followed the sequence below:

- Cleaning and drying of the core samples.
- Stabilize the air bath and all equipment at a temperature of 368.15 K for 24 hours.
- Saturated the core plugs with brine of 25,000 ppm.
- Displace brine with methane (90% composition).
- Record pressure response as a function of:
  - Injected pore volumes (including gas breakthrough),
  - Water saturation (including irreducible water saturation).
- Soxhlet extraction, to check final S_{wir} in the coreplug.

Direct measurement of in-situ water saturation (Sw) during flooding is technically challenging and impossible. Thus, material balance was the most practical and widely used approach for estimating Sw during dynamic displacement. Most importantly, to verify the material balance results, all core plugs were subjected to Soxhlet extraction after the experiment, and the resulting residual (irreducible) water saturation values matched the endpoint saturation predicted by the flooding data.

Subsequently, the produced microalgae were injected into the biocathode together with the microalgae cultivation medium, which is regarded as the catholyte. In this study, a BG11 medium was employed as the culture medium [14], which consisted of the following components (in grams per liter): 0.26 Na_2HPO_4, 0.74 KH_2PO_4, 0.01 $CaCl_2$, 0.01 Fe-EDTA, 0.05 $MgSO_4.7H_2O$, Na_2CO_3, and 1 ml trace elements. The microalgae that were used for this study were changed based on the ideal culture conditions, the required carbon source for the microalgae was CO_2, which was supplied by a CO_2 cylinder (purity of 99.99%). The required light for microalgae cultivation was provided by fluorescent lamps reported by Barahoei et al. [15]. The fluorescent lights were utilized to provide the requisite light for the growth of the microalgae.

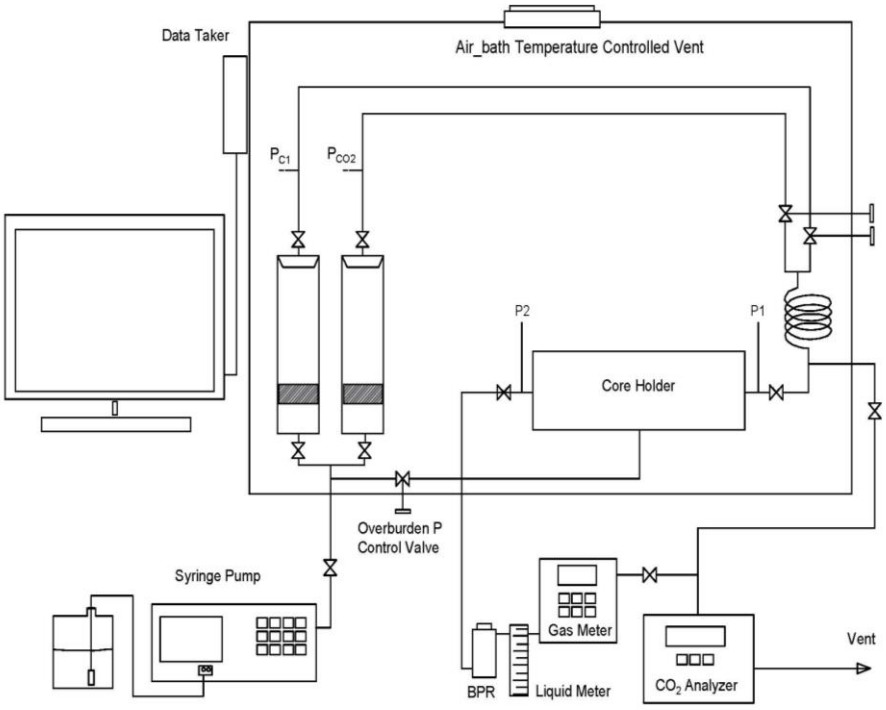

Fig. 1. Schematic diagram of the dynamic core flooding rig

4- Core plug properties

The reservoir rock properties of the core plug samples used in this study are presented in Table 1. A clear trend is observed, whereby both permeability and porosity decrease with increasing depth and there is a linear correlation between the absolute permeability and porosity of the core samples.

Table 1. Measured basic core plug petrophysical properties

S.N.	Sample Code	Depth (m)	K air (md)	Porosity (%)	PV (cc)
1	*C1*	4144.28	391	17.9	9.82
2	*C2*	4160.68	115	14.1	7.96
3	*C3*	4184.37	8.37	9.9	5.73

5- Fluid properties

The injected phase consisted of 90% methane and 10% carbon dioxide (CO_2). A PVT analysis of the injection mixture indicated a critical pressure and temperature of 5.66 MPa and 187.55 K, respectively. It is known that pure CO_2 reaches supercritical conditions at 304.15 K and 7.39 MPa. However, given that CO_2 constitutes only 10% of the injected phase, its influence on the overall thermophysical properties of the displacing fluid is minimal. Soxhlet extraction confirmed negligible gas dissolution effects on final irreducible water saturation.

Table 2 shows the petrophysical properties of core plugs measured under both ambient and reservoir conditions. Under ambient conditions, the liquid permeability of each sample is significantly lower than the corresponding gas permeability, primarily due to the gas slippage effect. In contrast, the effective gas permeability under reservoir conditions is significantly lower than the ambient air permeability. This reduction is attributed to the influence of overburden pressure, increased fluid viscosity, and the presence of a second phase within the pore structure. During the experiment, the displaced phase (brine) remained in the liquid state, while the injected phase was in the gaseous state at test conditions of ~ 41.37 MPa and 368.15 K. This indicates that the displacement occurred under immiscible conditions, with the injected gas phase displacing the in-situ aqueous phase.

Table 2. Ambient and reservoir condition core plug properties

Ambient Condition				Reservoir Condition (40.5 MPa and 368.15 K)	
S.N.	Samples Code	*K* air (md)	Porosity (%)	*Kw* (md)	Effective Gas *K* (md) *Kg@S_{wir}*
1	*C1*	391	17.9	10.84	70.4
2	*C2*	115	14.1	7.02	41.8
3	*C3*	8.37	9.9	2.71	24.2

6- Results and discussion

Capillary pressure (P_c) during gas-water coreflooding was measured to investigate fluid displacement behavior in sandstone core samples of varying quality under high-pressure and high-temperature (HPHT) conditions. P_c arises due to interfacial tension and the curvature of the gas-water interface within the porous medium. To ensure capillary-dominated flow and minimize viscous effects, the gas injection rate was kept low (~ 0.17 cc/min), allowing capillary forces to control the displacement process. As outlined in Section 5, the experimental sequence involved displacing brine-saturated core plugs with methane gas. Fig. 2 (a–c) illustrates P_c plotted against injected pore volume (PV) and water saturation (Sw). At the early stages of gas injection, gas preferentially invades the larger pores, where the entry capillary pressure is low due to the lower interfacial curvature. As gas continues displace brine and begins to enter smaller pores, the curvature of the gas–brine interface increases, leading to a corresponding increase in capillary pressure (Pc).

However, with continued injection, P_c rises again as the gas phase progresses into smaller and more resistive pore spaces. This secondary increase in P_c is observed in samples like C1 and also reported in recent literature [20–23] is attributed to the gas encountering smaller throats that require higher pressure to overcome entry resistance. After gas breakthrough, P_c gradually stabilizes, signalling a transition from capillary-dominated to viscous-dominated flow.

This behavior can also be interpreted in terms of pore size distribution. Sample *C1*, a high-quality rock with 17% porosity and permeability of 391 mD, exhibited an initial decline in capillary pressure after approximately 0.15 PV of injection, followed by a rise in P_c leading up to gas breakthrough. This trend suggests that *C1* likely contains larger pores, resulting in initially lower capillary pressures. As the injection pressure exceeds the capillary threshold in intermediate-sized pores, the non-wetting gas phase displaces the brine, causing a temporary drop in P_c.

A second rise in capillary pressure is observed after breakthrough, indicating gas invasion into smaller pores where higher capillary entry pressures are required. The variations in P_c reveal that while larger pores are effectively drained, water remains trapped in smaller pore spaces due to strong capillary forces. Around 0.8 PV, capillary pressure stabilizes, signifying a transition to steady-state flow dominated by viscous forces rather than capillary effects. A similar trend is observed in sample *C2*, representing intermediate rock quality. However, it requires a greater injected pore volume to reach the initial P_c rise and breakthrough, likely due to differences in pore size distribution, mineralogy, and heterogeneity.

$$Pc = P_{gas} - P_{brine} \quad (1)$$

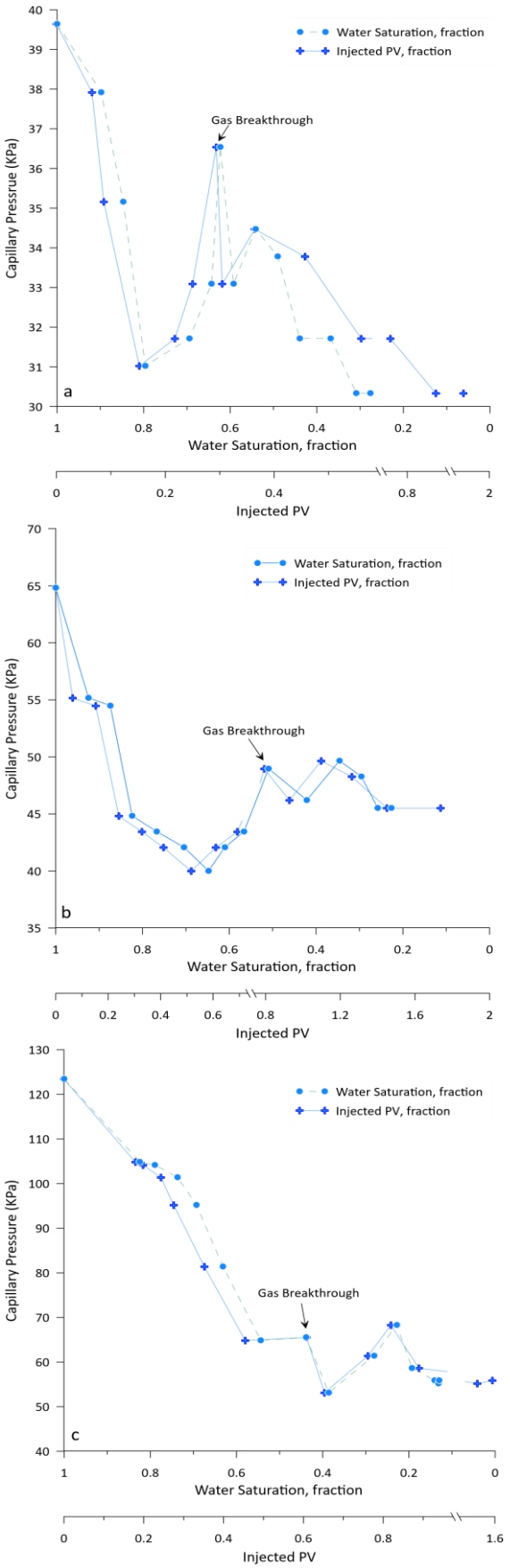

Fig. 2. Capillary pressure vs water saturation and injected gas PV for (a) Sample C1; (b) Sample C2; and (c) Sample C3

Sample *C3*, representing low-permeability rock, displayed a more gradual and consistent decline in P_c with injection, and a lower irreducible water saturation (S_{wir}) compared to *C1* and *C2*. This reflects increased water trapping in smaller pores due to stronger capillary forces. However, under HPHT conditions (~41.37 MPa and 368.15 K), irreducible water saturation values were lower than those typically observed at ambient conditions. This is due to reduced interfacial tension (IFT) at elevated temperature and pressure, allowing the pressure gradient across the core to exceed the capillary entry pressures of small pores. As a result, displacement efficiency improved, and more brine was expelled even from tighter pore spaces.

The capillary number (Eq. 2) plays a critical role in this behavior. At HPHT, the increase in Cn, even at modest injection rates, may have s promoted piston-like displacement and reducing S_{wir}, particularly in tight rocks like *C3*. Furthermore, capillary fingering likely occurred in Sample *C3*, which is a low-permeability and low-porosity sample. This is consistent with Lenormand et al. (1988)'s observations, where capillary-dominated flow at low capillary numbers leads to irregular displacement fronts. This may explain the residual brine saturation and non-monotonic *Pc–Sw* behavior observed. This emphasizes the importance of conducting P_c and relative permeability measurements under reservoir-representative conditions, where dynamic methods can capture the real interplay of capillary and viscous forces across a range of pore structures.

$$C_n = {\mu v}/{\sigma} \quad (2)$$

μ viscosity of the phase, *Pa.s*, *v* velocity of the phase, *m/s*
σ interfacial tension, *N/m.*

Understanding how capillary forces control fluid displacement across different rock qualities is key to predicting gas recovery and irreducible water saturation. Reduced water trapping under HPHT conditions, due to lower interfacial tension and higher viscous dominance, implies ambient-condition tests may underestimate productivity. The transition from capillary to viscous-dominated flow and observed non-monotonic pressure behavior in tight rocks emphasize the need for reservoir-representative measurements to evaluate residual saturation and recoverable gasanalysis.

7- Conclusion

This study addresses a significant gap in the literature by presenting laboratory results on capillary pressure (Pc) measurements at high pressure and temperature (HPHT). Dynamic coreflooding experiments were conducted on reservoir sandstone core plugs retrieved from a gas field in Australia. The injection rate (~0.3 cc/min), pore pressure (~41.37 MPa), and temperature (368.15 K) were precisely controlled throughout the experiments. The primary objective was to derive accurate Pc–Sw relationships under reservoir-representative conditions while avoiding semipermeable membrane end effects. Flow was tightly controlled using a needle valve to maintain quasi-static displacement and minimize viscous forces. The key findings from this research include:

- Reliable Pc curves were obtained across core plugs with varying permeability and porosity.
- Secondary Pc peaks suggest gas entry into smaller pores after breakthrough.
- Variations in S_{wir} reflect differences in pore structure and wettability.
- Capillary fingering likely occurred in low-permeability sample *C3* under low-C_n conditions.
- Soxhlet extraction confirmed negligible gas dissolution effects on final Sw.

Under such high-pressure, high-temperature, and low-flow quasi-static conditions, the viscous pressure drop is negligible, and the measurement of capillary pressure becomes much more stable and representative. In fact, introducing a porous plate in this setting could introduce a strong End Effect, particularly where it's the pore diameter is smaller than that of the core. In such cases, the pressure buildup required for displacement will reflect the capillary entry pressure of the plate, not of the rock, and may skew the results.

Gas dissolution effects were negligible, as confirmed by Soxhlet extraction. Core-scale heterogeneity remains a limitation, but representative samples were chosen to reflect dominant reservoir features.

Acknowledgment

The author gratefully acknowledges the financial support from Shell Australia for this research program. Special thanks are also extended to Dr. Arsalan Ahmed of Komar University of Science and Technology for his invaluable assistance with data analysis.

References

[1] R. T. Armstrong, M. L. Porter and D. Wildenschild, "Linking pore-scale interfacial curvature to column-scale capillary pressure," *Advances in Water Resources*, vol. 46, pp. 55-62, 2012, https://doi.org/10.1016/j.advwatres.2012.05.009

[2] J. S. Ward and N. R. Morrow, "Capillary Pressures and Gas Relative Permeabilities of Low-Permeability Sandstone," *SPE Formation Evaluation*, pp. 345-356, 1987, https://doi.org/10.2118/13882-PA

[3] W. Song, J. Yao, K. Zhang, Y. Yang and H. Sun, "Understanding gas transport mechanisms in shale gas reservoir: Pore network modelling approach," *Advances in Geo-Energy Research*, vol. 6, no. 4, pp. 359-360, 2022, https://doi.org/10.46690/ager.2022.04.11

[4] Y. Xiao, Y. He, J. Zheng and J. Zhao, "Modeling of two-phase flow in heterogeneous wet porous," *Capillarity*, vol. 5, no. 3, pp. 41-50, 2022, https://doi.org/10.46690/capi.2022.03.01

[5] S. T. Hussain, K. Regenauer-Lieb, A. Zhuravljov, F. Hussain and S. S. Rahman, "The impact of wettability and fluid saturations on multiphase representative elementary volume estimations of micro-porous media," *Capillarity*, vol. 9, no. 1, pp. 1-8, 2023, https://doi.org/10.46690/capi.2023.10.01

[6] Y. Li, H. Luo, H. Li, S. Chen, X. Jiang and J. Li, "Dynamic capillarity during displacement process in fractured tight reservoirs with multiple fluid viscosities," *Energy Science & Engineering*, vol. 8, pp. 300-311, 2019, https://doi.org/10.1002/ese3.558

[7] Y. Li, H. Li, J. Cai, Q. Ma and J. Zhang, "The dynamic effect in capillary pressure during the displacement process in ultra-low permeability sandstone reservoirs," *Capillarity*, vol. 1, no. 2, pp. 11-18, 2018, https://doi.org/10.26804/capi.2018.02.01

[8] D. B. Das and M. Mirzaei, "Dynamic effects in capillary pressure relationships for two-phase flow in porous media: Experiments and numerical analyses," *AIChE Journal*, vol. 58, no. 12, pp. 3891-3900, 2012, https://doi.org/10.1002/aic.13777

[9] Y. Li, H. Luo, H. Li, X. Liu, Y. Tan, S. Chen and J. Cai, "A brief review of dynamic capillarity effect and its characteristics in low permeability and tight reservoirs," *Journal of Petroleum Science and Engineering*, vol. 189, 2020, https://doi.org/10.1016/j.petrol.2020.106959

[10] Q. Lin, B. Bijeljic, H. Rieke and M. J. Blunt, "Visualization and quantification of capillary drainage in the pore space of laminated sandstone by a porous plate method using differential imaging X-ray microtomography," *Water Resources Research*, pp. 7457-7468, 2017, https://doi.org/10.1002/2017WR021083

[11] I. Shikhov and C. H. Arns, "Evaluation of Capillary Pressure Methods via Digital Rock Simulations," *Transport in Porous Media*, vol. 107, no. 2, pp. 623-640, 2015, https://doi.org/10.1007/s11242-015-0459-z

[12] J. Kamath and C. Laroche, "Laboratory-Based Evaluation of Gas Well Deliverability Loss Caused by Water Blocking," *SPE*, vol. 8, no. 01, pp. 71-80, 2003, https://doi.org/10.2118/83659-PA

[13] J. Mahadevan, M. M. Sharma and Y. C. Yortsos, "Evaporative Cleanup of Water Blocks in Gas Wells," *SPE*, 2005, https://doi.org/10.2118/94215-MS

[14] T. Rahman, M. Lebedev, A. Barifcani and S. Iglauer, "Residual trapping of supercritical CO_2 in oil-wet sandstone," *Journal of Colloid and Interface Science*, vol. 469, pp. 63-68, 2016, https://doi.org/10.1016/j.jcis.2016.02.020

[15] X. Liu, Y. Kang, J. LiZhanjun, ChenAnzhao and J. Xu, "Percolation Characteristics and Fluid Movability Analysis in Tight Sandstone Oil Reservoirs," *ACS Omega*, vol. 5, no. 24, pp. 14316-14323, 2020, https://doi.org/10.1021/acsomega.0c00569

[16] R. S. Mohammad, M. Y. K. Tareen, A. Mengel, S. A. R. Shah and J. Iqbal, "Simulation study of relative permeability and the dynamic capillarity of waterflooding in tight oil reservoirs," *Journal of Petroleum Exploration and Production Technology*, vol. 10, pp. 1891-1896, 2020, https://doi.org/10.1007/s13202-020-00856-x

[17] H. Sidiq and R. Amin, "Impact of pore-pressure on the recovery efficiency from CO_2-methane displacement experiments," *IEEE Workshop on Environmental Energy and Structural Monitoring Systems, Taranto, Italy*, 2010, pp. 1-8, https://doi.org/10.1109/EESMS.2010.5634175

[18] H. Sidiq, R. Amin, E. Van der Steen, T. Kennaird, "Super critical CO_2–methane relative permeability investigation," *Journal of Petroleum Science and Engineering*, vol. 78, no. 3-4, pp. 654-663, 2011, https://doi.org/10.1016/j.petrol.2011.08.018

[19] M. N. Mahmood, V. Nguyen, B. Guo, "Challenges in mathematical modeling of dynamic mass transfer controlled by capillary and viscous forces in spontaneous fluid imbibition processes," *Capillarity*, vol. 11, no. 2, pp. 53-62, 2024, https://doi.org/10.46690/capi.2024.05.03

[20] M. Andrew, B. Bijeljic, M. J. Blunt, "Pore-by-pore capillary pressure measurements using X-ray microtomography at reservoir conditions: Curvature, snap-off, and remobilization of residual CO_2," *Water Resources Research*, vol. 50, no. 11, pp. 8760-8774, 2014, https://doi.org/10.1002/2014WR015970

[21] A. L. Herring, C. Sun, R. T. Armstrong, Z. Li, J. E. McClure, M. Saadatfar, "Evolution of Bentheimer Sandstone Wettability During Cyclic scCO_2-Brine Injections," *Water Resources Research*, vol. 57, no. 11, pp. 1-22, 2021, https://doi.org/10.1029/2021WR030891

[22] Y. Cao, M. Tang, Q. Zhang, J. Tang, S. Lu, "Dynamic capillary pressure analysis of tight sandstone based on digital rock model," *Capillarity*, vol. 3, no. 2, pp. 28-35, 2020, https://doi.org/10.46690/capi.2020.02.02

[23] Y. Li, C. Liu, H. Li, S. Chen, K. Lu, Q. Zhang and H. Luo, "A review on measurement of the dynamic effect in capillary pressure," *Journal of Petroleum Science and Engineering*, vol. 208, 2022, https://doi.org/10.1016/j.petrol.2021.109672

دراسة تجريبية لقياس الخاصية الشعيرية بين الغاز والمحلول الملحي عند درجات الحرارة والضغوط المرتفعة

هيوا صديق [١، *]

١ قسم هندسة البترول، كلية الهندسة، جامعة كومار للعلوم والتكنولوجيا، السليمانية، العراق

الخلاصة

يُعدّ فهم منحنيات الضغط الشعيري أثناء تجارب الإزاحة المتبادلة بين الغاز والمحلول الملحي في العينات الصخرية أمرًا أساسيًا لتحليل سلوك الموائع في الأوساط المسامية، ولا سيّما في المكامن الغازية. تعتمد عملية القياس المباشر للضغط الشعيري في تجارب الإزاحة الديناميكية على تقييم التوازن بين القوى الشعرية وتدرجات الضغط داخل البنية المسامية. في هذه الدراسة التجريبية، تم اخذ ثلاث عينات صخرية من مكمن غازي طبيعي يقع في الجرف الشمالي الغربي لأستراليا. أُجريت التجارب في ظروف تحاكي ظروف المكمن الحقيقي (حوالي 41.37ميكا باسكال و 368.15 كلفن) بهدف دراسة تأثير حجم المسام والمسامية والتشبع المائي على منحنى الضغط الشعيري.

أظهرت منحنيات الضغط الشعيري للعينات (C1–C3) سلوكيات ديناميكية مميزة؛ إذ أبدت العينتان C1 وC2، واللتان تمتازان بنفاذية ومسامية عاليتين، انخفاضًا أوليًا أعقبه ارتفاع متزايد في الضغط الشعيري حتى لحظة الاختراق. في المقابل، أظهرت العينة C3، والتي تمتاز بنفاذية ومسامية منخفضتين، تشبعًا مائيًا أقل. رغم ذلك، فمن المتوقع عادة وجود تشبع اعلى للمحلول الملحي في العينات ذات المسامية المنخفضة نتيجة ازدياد مساحة سطح الحبيبات وصِغَر ممرات المسام التي تحتجز مرحلة البلّل. يُعزى هذا السلوك غير المتوقع إلى إجراء التجارب في ظروف ضغط وحرارة مرتفعتين. تؤكد هذه النتائج الدور الحاسم لهندسة المسام في التحكم بكفاءة الإزاحة والاحتجاز الشعيري. كما توفر رؤى كمية مهمة لنمذجة المكامن، ولا سيما في التنبؤ باسترجاع الغاز في ظروف الضغط والحرارة العاليتين، حيث تكون القوى الشعرية ذات تأثير ملحوظ.

الكلمات الدالة: الضغط الشعيري، الإزاحة في العينات الصخرية، الضغط والحرارة العاليان، المكمن الغازي.